RESEARCH ARTICLE

Greenland surface air temperature changes from 1981 to 2019 and implications for ice-sheet melt and mass-balance change

Edward Hanna[1] | John Cappelen[2] | Xavier Fettweis[3] |
Sebastian H. Mernild[4,5,6,7] | Thomas L. Mote[8] | Ruth Mottram[2] |
Konrad Steffen[9] | Thomas J. Ballinger[10] | Richard J. Hall[11]

[1]School of Geography and Lincoln Centre for Water & Planetary Health, University of Lincoln, Lincoln, UK

[2]Danish Meteorological Institute, Copenhagen, Denmark

[3]SPHERES research unit, Geography, University of Liège, Liège, Belgium

[4]Nansen Environmental and Remote Sensing Center, Bergen, Norway

[5]Faculty of Engineering and Science, Western Norway University of Applied Sciences, Sogndal, Norway

[6]Direction of Antarctic and Sub-Antarctic Programs, Universidad de Magallanes, Punta Arenas, Chile

[7]Geophysical Institute, University of Bergen, Bergen, Norway

[8]Department of Geography, University of Georgia, Athens, Georgia

[9]Swiss Federal Institute for Forest, Snow and Landscape Research WSL, Birmensdorf, Switzerland

[10]International Arctic Research Center, University of Alaska Fairbanks, Fairbanks, Alaska

[11]School of Geographical Sciences, University of Bristol, Bristol, UK

Correspondence
Edward Hanna, School of Geography, University of Lincoln, Think Tank, Ruston Way, Lincoln LN6 7FL, UK.
Email: ehanna@lincoln.ac.uk

Abstract

We provide an updated analysis of instrumental Greenland monthly temperature data to 2019, focusing mainly on coastal stations but also analysing ice-sheet records from Swiss Camp and Summit. Significant summer (winter) coastal warming of $\sim$1.7 (4.4)°C occurred from 1991–2019, but since 2001 overall temperature trends are generally flat and insignificant due to a cooling pattern over the last 6–7 years. Inland and coastal stations show broadly similar temperature trends for summer. Greenland temperature changes are more strongly correlated with Greenland Blocking than with North Atlantic Oscillation changes. In quantifying the association between Greenland coastal temperatures and Greenland Ice Sheet (GrIS) mass-balance changes, we show a stronger link of temperatures with total mass balance rather than surface mass balance. Based on Greenland coastal temperatures and modelled mass balance for the 1972–2018 period, each 1°C of summer warming corresponds to $\sim$(91) 116 Gt·yr^{-1} of GrIS (surface) mass loss and a 26 Gt·yr^{-1} increase in solid ice discharge. Given an estimated 4.0–6.6°C of further Greenland summer warming according to the regional model MAR projections run under CMIP6

future climate projections (SSP5-8.5 scenario), and assuming that ice-dynamical losses and ice sheet topography stay similar to the recent past, linear extrapolation gives a corresponding GrIS global sea-level rise (SLR) contribution of ~10.0–12.6 cm by 2100, compared with the 8–27 cm (mean 15 cm) "likely" model projection range reported by IPCC in 2019 (SPM.B1.2). However, our estimate represents a lower limit for future GrIS change since fixed dynamical mass losses and amplified melt arising from both melt-albedo and melt-elevation positive feedbacks are not taken into account here.

1 | INTRODUCTION

Recent research highlights increased mass loss from the Greenland Ice Sheet (GrIS) (Shepherd et al., 2020; Hanna et al., 2013a; Hanna et al., 2020; Bamber et al., 2018), and the ice sheet's response to anthropogenic global warming includes a non-linear effect of rising air temperatures on melt and runoff (Trusel et al., 2018). Trusel et al. (2018) found a 250–575% increase in melt intensity at multiple ice-core sites in the Jakobshavn drainage basin on the west flank of the GrIS during 1994–2013, which corresponds with a period of strong global warming influence on Greenland surface air temperatures (Hanna et al., 2012). Recent extreme melt events in summers 2012 (Nghiem et al., 2012; Tedesco et al., 2013; Hanna et al., 2014) and 2019 (NSIDC, 2019; Tedesco and Fettweis, 2020) highlight the high sensitivity of GrIS to climate change, and its potential proximity to a tipping point (Lenton et al., 2008; Box et al., 2018; Pattyn et al., 2018), especially since large areas of the ice-sheet margins, and inland areas tend to be around or sometimes well above 0°C in summer (Hanna and Cappelen, 2002; Hanna and Braithwaite, 2003; Trusel et al., 2018). Apart from annual snapshots of yearly extremes published in NOAA's Arctic Report Card, Greenland section (Tedesco et al., 2019), the last systematic seasonal analyses of coastal and inland Greenland in situ instrumental air temperature records were published by Hanna et al. (2012) and Mernild et al. (2013), although Ogi et al. (2016), Abermann et al. (2017) and Ballinger et al. (2018) present some coastal temperature analyses that extend to 2013 or 2014. Here we present an updated analysis of both coastal and inland temperature records, focusing on seasonal temperature trends, and the unusually warm summer of 2019 in comparison with the record warm 2012 Greenland summer. Since Greenland summer temperature changes are crucial for affecting GrIS mass balance and global sea-level rise, we also explore the relation between these parameters for both recent (1972–2018) and future (until 2100) climate conditions based on the output of a regional climate model (MAR) forced by the latest available (CMIP6) suite of global climate model (GCM) predictions.

2 | DATASETS AND METHODS

We use updated, quality-controlled monthly surface air temperature data from Danish Meteorological Institute (DMI) synoptic stations (Cappelen, 2020), Greenland Climate Network (GC-Net; Steffen and Box, 2001) automatic weather stations (AWS) Swiss Camp (1169-m elevation, western flank of GrIS) and Summit (3200-m elevation in centre of GrIS), and an AWS located at 515-m elevation on a nunatak next to Mittivakkat Gletscher (Gl.) on Ammassalik Island in south-east Greenland (Figure 1). The DMI data and Mittivakkat Gl. series are updated through December and August 2019 respectively, while the GC-Net AWS records are available to April 2019 and are updated from the time series presented in Hanna et al. (2014). We supplement the DMI and GC-Net Summit station records with NOAA GEOSummit data for 2019, available from: ftp://ftp.cmdl.noaa.gov/met/sum/. Full details of the corrections applied in the construction of the DMI and Swiss Camp and Summit temperature series are given in Hanna et al. (2014); for example, the main (DMI) dataset has been pre-checked for temporal coverage and homogeneity (Cappelen, 2020). Following Hanna et al. (2012, 2013b) we use Composite Greenland Temperatures CGT2 and CGT3, which are monthly means of respectively nine (Upernavik, Aasiaat, Ilulissat, Sisimiut, Nuuk, Paamiut, Narsarsuaq, Qaqortoq and Tasiilaq) and five overlapping (Upernavik, Ilulissat, Nuuk, Narsarsuaq and Tasiilaq) DMI coastal Greenland stations (Figure 1). These averages extend back to 1961 and 1895 respectively.

FIGURE 1 Map showing weather stations used in this study. CGT2 (CGT3) stations are depicted by red squares and blue asterisks (blue asterisks). The 5-digit numbers refer to the World Meteorological Organization station codes [Colour figure can be viewed at wileyonlinelibrary.com]

Trend analysis is conducted based on linear least-squares regression and significance testing, with results regarded as statistically significant at $p \leq 0.05$. Correlation analysis, also with significance testing, is based on de-trended time series. Standard meteorological seasons are used, so DJF = winter, MAM = spring, JJA = summer and SON = autumn, where winter follows the year of January. Following Turner *et al.* (2016), we also calculated temperature trends using the Mann-Kendall Tau and Sen's slope test, together with confidence intervals, in order to identify breakpoints that may mark times of significant temperature (trend) change.

For analysing the association between Greenland temperature and atmospheric circulation changes over the Greenland region, we use Hurrell's principal-component-based North Atlantic Oscillation (NAO) monthly series (available online at https://climatedataguide.ucar.edu/climate-data/hurrell-north-atlantic-oscillation-nao-index-pc-based) (Hurrell, 1995) and Greenland Blocking Index (GBI) monthly and daily data (https://www.esrl.noaa.gov/psd/gcos_wgsp/Timeseries/GBI_UL/; https://www.esrl.noaa.gov/psd/data/timeseries/daily/GBI/) showing anomalies and changes in mid-tropospheric anticyclonic conditions over the Greenland region (Hanna

et al., 2013b; Hanna *et al.*, 2016; Hanna *et al.*, 2018a). The GBI is the area-weighted mean 500 hPa geopotential height field calculated over the following domain: 60–80°N, 20–80°W.

Observations of satellite-derived surface melt extent and duration are derived from brightness temperatures measured by the Special Sensor Microwave Imager/Sounder (SSMIS) passive microwave radiometer (Mote, 2007; Tedesco *et al.*, 2013). Near real time SSMIS brightness temperatures on a 25-km polar stereographic grid are available from the National Snow and Ice Data Center (NSIDC) (Maslanik and Stroeve, 1999). The surface melt identification method uses a dynamic threshold of 19 GHz, horizontally polarized, brightness temperatures derived from a microwave emission model of firn conditions associated with at least 1% liquid water content (Mote and Anderson, 1995). Melt is observed when brightness temperatures exceed the threshold for a given location. Output is re-gridded to the equal area EASE2 25-km grid prior to calculation of melt extent, consistent with the historical climate data record of melt extent maintained by NSIDC (Mote, 2014).

For comparing recent changes in Greenland temperatures with GrIS mass balance, surface mass balance (snow accumulation minus surface meltwater runoff) and solid-ice discharge variations, we use the recently-published dataset of Mouginot *et al.* (2019). This is based on the mass-budget method using an optimized, down-scaled regional climate model and spatially-/temporally-enhanced aerial, satellite and bathymetric datasets (Mouginot *et al.*, 2019).

Future projections made for the Ice Sheet Model Intercomparison Project for CMIP6 (ISMIP6) (Nowicki *et al.*, 2016) by the regional climate model MAR (Fettweis *et al.*, 2017) forced by the new CMIP6 "high end" (update of RCP8.5) scenario (SSP5-8.5; O'Neill *et al.*, 2016) until 2100 are used here to estimate warming rates over Greenland for the next decades. Version 3.9 of MAR is used here at a resolution of 15 km, and was forced at 6-hour timesteps by five Earth System Models (CESM2, CNRM-CM6-1, CNRM-ESM2-1, MRI-ESM2-0 and UKESM1-0-LL) from the CMIP6 database. We refer to Fettweis *et al.* (2017) for a more detailed description of MAR, and to Delhasse *et al.* (2020) for the validation of MARv3.9. The MAR model, forced by NCEP-NCARv1 (1950–2019) and ECMWF ERA-40 (1958–1978) and ERA-5 (1979–2019) reanalysis data using the set-ups of Fettweis *et al.* (2017) and Fettweis *et al.* (2020) (respective grid resolutions of 20 km and 15 km), is also used to map the recent observed warming over the GrIS.

Figures S1 and S2 respectively compare the mean annual SMB and mean summer (JJA) near surface air temperature for 1981–2010, calculated using MAR forced by the five CMIP6 models, with that simulated by MAR forced by ERA5 [which is the MAR simulation extensively validated in Fettweis *et al.*, 2020]. For SMB, differences greater than the standard deviation (SD) of MAR-ERA5 (as a measure of interannual variability) are hatched. Differences can be large locally but remain statistically insignificant in most areas. When integrated over the whole ice sheet (Table 1), these differences do not greatly impact the reliability of the future projections. When compared with the CMIP5-driven MAR simulations (Fettweis *et al.*, 2013), MAR driven by CMIP6 is generally better for current climate.

We have added the interannual variability (*SD* around the mean over each period) in Table 1 to show where the differences of CMIP6- versus reanalysis-based MAR runs are significant. For 1972–1990 the differences are lower than the interannual variability. Over 2001–2019, the CMIP6-forced MAR simulations systematically overestimate SMB and underestimate melt because the recent general circulation changes in summer (increase of blocking events) driving the recent melt increase are not represented by the global models. As shown by Delhasse *et al.* (2018), accounting for circulation changes in the GCM-driven projections would amplify simulated melt and reduce SMB, bringing these parameters into better agreement with the reanalysis reconstructions for 2001–2019.

3 | GREENLAND TEMPERATURE ANALYSIS AND INTERPRETATION

3.1 | Temperature trends

During 1991–2019 there was significant overall warming of ~4.4°C in winter, ~2.7°C in spring, and ~1.7°C in summer, that was generally focused in areas away from the extreme south (Table 2; Figure 2a–d). Autumn coastal trends since 1991 are only locally significant and are focused in northeast and east Greenland (especially Danmarkshavn). The strongest warming was in west and northwest Greenland, up to ~6–6.5°C in winter. For the overall 1981–2019 period these values reach ~6–7.5°C. However, mean temperature trends are not significant for all seasons since 2001. This reflects a strong rise in coastal Greenland temperatures from the early 1990s until the early 2010s, with stabilization or slight decline thereafter, although this is not a significant change according to Mann-Kendall testing and therefore most likely reflects natural variability. Summer and July temperature trends for 1991–2018 at Swiss Camp are respectively 1.7°C and 1.2°C (Figure 3), which are significant warmings and broadly comparable with 1.5/1.6°C for

TABLE 1 Greenland Ice Sheet mean summer temperature (°C) and mean annual melt, runoff and SMB values (Gt·yr^{-1}) for two recent past periods from Mouginot *et al.* (2019), MAR/NCEP and MAR/ECMWF Reanalyses, and for the same periods and the late Twentieth Century as modelled using MAR and CMIP6 using the SSP5-8.5 scenario (O'Neill *et al.*, 2016). For each parameter/period, the numbers in brackets show the standard deviation (interannual variability) based on the respective yearly values

Model/forcing	Parameter	1972–1990	2001–2019 (2001–2018 for Mouginot and MAR/ECMWF data)	2081–2099
Mouginot *et al.* (2019)	SMB	442.5 (98.4)	271.8 (91.4)	N/A
MAR/NCEP	Temperature	−7.9 (0.5)	−6.7 (0.7)	N/A
	Melt	402.6 (58.6)	601.8 (148.9)	N/A
	Runoff	249.6 (47.0)	402.2 (102.6)	N/A
	SMB	433.9 (104.1)	288.2 (107.9)	N/A
MAR/ECMWF	Temperature	−8.1 (0.6)	−6.9 (0.7)	N/A
	Melt	386.9 (64.2)	591.6 (141.5)	N/A
	Runoff	223.8 (49.2)	386.8 (101.2)	N/A
	SMB	498.4 (113.0)	319.0 (109.1)	N/A
MAR/CESM2	Temperature	−8.2 (0.6)	−6.6 (0.8)	−1.0 (0.8)
	Melt	346.3 (65.0)	588.7 (134.7)	2,603.8 (522.2)
	Runoff	180.7 (35.0)	370.7 (96.1)	2,234.9 (526.0)
	SMB	516.4 (72.4)	399.8 (134.5)	−1,265 (501.9)
MAR/CNRM-CM6	Temperature	−8.6 (0.6)	−7.7 (0.7)	−2.4 (1.0)
	Melt	355.0 (68.9)	474.8 (98.9)	1924.5 (374.5)
	Runoff	233.1 (52.3)	322.0 (72.3)	1,670.3 (372.9)
	SMB	520.3 (75.9)	473.2 (103.9)	−652.8 (296.1)
MAR-CNRM-ESM2	Temperature	−9.0 (0.7)	−7.8 (0.5)	−2.7 (0.6)
	Melt	355.4 (80.0)	506.5 (67.5)	1790.6 (292.1)
	Runoff	227.6 (60.8)	354.3 (53.1)	1,530.1 (296.2)
	SMB	419.8 (97.0)	358.2 (94.0)	−670.8 (248.5)
MAR-MRI-ESM2	Temperature	−7.9 (0.6)	−6.5 (0.8)	−2.5 (0.6)
	Melt	427.7 (81.9)	617.1 (117.7)	1,659.4 (188.4)
	Runoff	258.4 (59.6)	403.7 (82.5)	1,355.9 (176.4)
	SMB	495.4 (101.5)	377.9 (85.4)	−380.6 (208.1)
MAR_UKESM1-CM6	Temperature	−9.6 (0.8)	−7.5 (0.7)	−0.9 (0.4)
	Melt	259.7 (105.0)	497.5 (100.6)	2,716.3 (360.2)
	Runoff	125.1 (61.1)	317.6 (66.0)	2,437.4 (353.3)
	SMB	512.6 (82.1)	427.6 (100.0)	−1,280.1 (332.2)

CGT2(3) for both July and summer (1991–2018). A similar significant warming of 1.9°C is observed at Summit for summer 1992–2019 (Figure 4). The observed summer warming of 1.1°C at Mittivakkat Gl. Nunatak from 1994–2019, with one missing year of data (2007), is based on a slightly shorter record and is not quite statistically significant. However, Greenland warming in summer since the early 1990s is generally significant and extends from the coastline across the ice sheet.

To determine possible physical insights into causes of these temperature changes (e.g., cloud-cover and radiation changes), we repeated the DMI station analysis on monthly mean minimum (parameter 111) and monthly mean maximum (parameter 121) surface air temperature changes, although fewer stations have complete records for these auxiliary measures of temperature (Tables 3 and 4; Figure 2). Temperature trends are not greatly different, although tend to be less significant overall, for the limited number of stations available. Summer trends for 1991–2019 are greater for mean maximum than mean minimum temperature, for example, 1.4°C versus 0.6°C for Kangerlussuaq, 3.4°C versus 1.7°C for

TABLE 2   Seasonal trends in *mean* (DMI parameter 101) daily air temperature at DMI coastal stations and CGT averages for various periods to 2019

Station WMO code	DJF (1981–2019)	DJF (1991–2019)	DJF (2001–2019)	MAM (1981–2019)	MAM (1991–2019)	MAM (2001–2019)	JJA (1981–2019)	JJA (1991–2019)	JJA (2001–2019)	SON (1981–2019)	SON (1991–2019)	SON (2001–2019)
Upernavik	**7.0**	**5.2**	*−2.4*	**<u>3.7</u>**	**3.5**	*0.2*	**2.2**	**<u>2.4</u>**	*−0.3*	**2.0**	*1.1*	*−0.4*
Aasiaat	**7.6**	**6.4**	*−1.0*	**<u>5.7</u>**	**4.9**	*−0.5*	**<u>2.7</u>**	**<u>2.2</u>**	*0.1*	**<u>2.0</u>**	**1.3**	*−0.4*
Ilulissat	**<u>5.8</u>**	**<u>4.9</u>**	*−0.8*	**<u>4.2</u>**	**4.6**	*0.1*	*1.0*	*1.0*	*−0.6*	*1.2*	*0.1*	*−1.1*
Sisimiut	**<u>7.1</u>**	**<u>6.3</u>**	*−1.3*	**<u>4.3</u>**	**3.3**	*−0.9*	**<u>3.0</u>**	**<u>2.7</u>**	*−0.4*		*−0.1*	*−1.0*
Kangerlussuaq	**4.7**	*3.2*	*−1.1*	**<u>4.3</u>**	*3.3*	*0.8*	**2.0**	**1.5**	*0.3*	*1.4*	*0.7*	*−1.2*
Nuuk	**3.3**	**3.0**	*−1.4*	**2.5**	*1.8*	*−0.6*	**<u>2.8</u>**	**<u>2.6</u>**	*0.7*	**1.6**	**1.5**	*−1.0*
Paamiut	**3.6**	**4.3**	*0.4*	**2.5**	*1.6*	*−1.3*	**2.0**	*1.0*	*−0.6*	**2.2**	*1.1*	*0.0*
Narsarsuaq	**4.1**	**4.4**	*−0.8*	**<u>3.5</u>**	*2.1*	*−0.5*	**<u>1.6</u>**	*1.1*	*0.3*	**1.4**	*1.0*	*−0.6*
Qaqortoq	**3.5**	**3.5**	*−1.0*	**<u>2.5</u>**	*1.2*	*−1.1*	**<u>1.6</u>**	*0.4*	*−0.4*	**<u>1.8</u>**	*1.0*	*−0.7*
Danmarkshavn	**<u>3.1</u>**	**3.2**	*0.8*					**1.4**	*0.4*		**2.9**	*1.9*
Ittoqqortoormiit	**4.4**	**2.8**	*1.7*	**1.8**	*0.0*	*0.7*		*0.7*	*−0.1*		**1.8**	*1.3*
Tasiilaq	**<u>4.2</u>**	**3.1**	*1.1*	**<u>3.2</u>**	**1.7**	*0.3*	**2.2**	**<u>1.4</u>**	*−0.1*	**2.4**	**<u>1.5</u>**	*0.4*
Ikerasassuaq								**<u>1.5</u>**	*−0.2*			
CGT2	**<u>5.1</u>**	**4.6**	*−0.8*	**3.6**	**2.7**	*−0.5*	**2.1**	**1.6**	*−0.1*	**1.9**	*1.1*	*−0.5*
CGT3	**4.9**	**4.1**	*−0.9*	**3.4**	**2.7**	*−0.1*	**1.9**	**<u>1.7</u>**	*0.0*	**1.7**	*0.9*	*−0.6*

Notes: Significant trends of $p \leq 0.05$ (≤ 0.01) are in bold (bold + underline). Trends that are not significant are shown in italic.

FIGURE 2 Mean (a–d) daily, (e–h) mean maximum daily and (i–l) mean minimum daily air temperature (°C) for selected Greenland coastal stations and CGT2 averages from 1981 to 2019: (a,e,i) MAM; (b,f,j) JJA; (c,g,k) SON; (d,h,l) DJF [Colour figure can be viewed at wileyonlinelibrary.com]
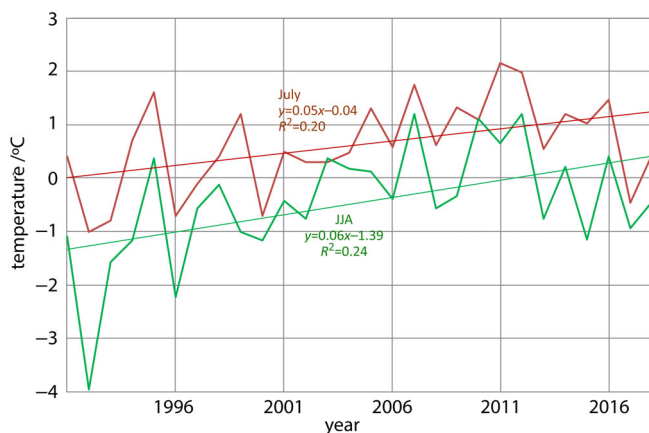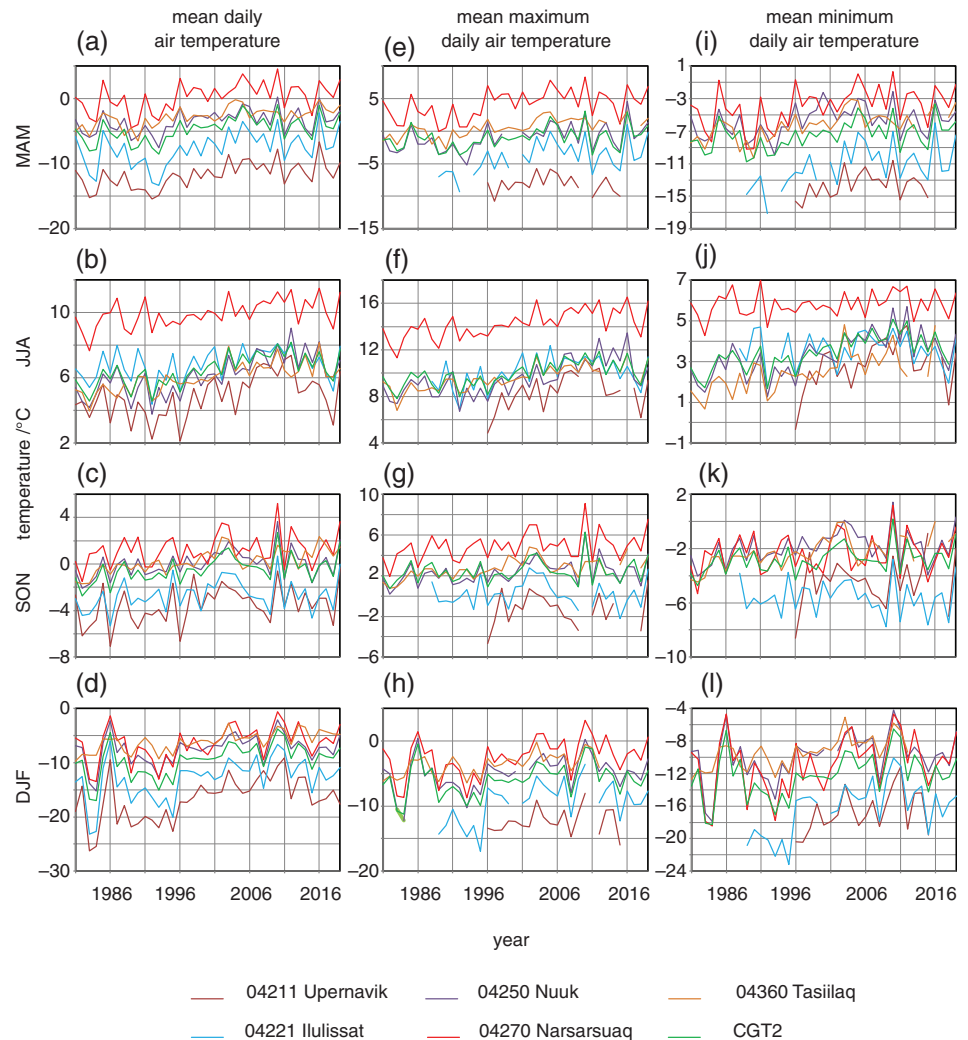

FIGURE 3 Summer (JJA) and July mean surface air temperature for 1991–2018 at GC-Net Swiss Camp, Greenland [Colour figure can be viewed at wileyonlinelibrary.com]
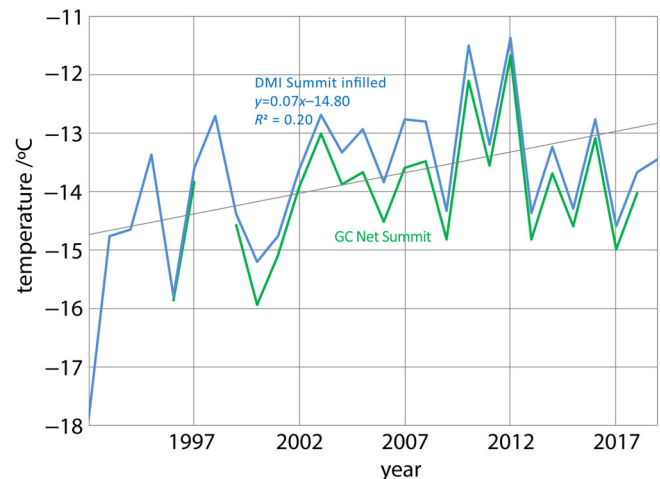

FIGURE 4 Summer (JJA) mean surface air temperature for 1992–2019 at Summit, Greenland: GC-Net and our synthesized Summit record (based on DMI data, infilled where latter are missing by regression fitting from GC-Net Summit data), updated from Hanna et al. (2012) [Colour figure can be viewed at wileyonlinelibrary.com]

Nuuk and 1.9°C versus 0.3°C for Narsarsuaq. This difference suggests an increased prevalence of clear skies and enhanced solar radiation in mainly boosting daytime

TABLE 3   Seasonal trends in Greenland *mean maximum* (DMI parameter 111) daily air temperature at DMI coastal stations and CGT averages for various periods to 2019

| Station WMO code	DJF (1981–2019)	DJF (1991–2019)	DJF (2001–2019)	MAM (1981–2019)	MAM (1991–2019)	MAM (2001–2019)	JJA (1981–2019)	JJA (1991–2019)	JJA (2001–2019)	SON (1981–2019)	SON (1991–2019)	SON (2001–2019)
Aasiaat	**7.1**	**5.6**	*-0.8*				**2.5**	**2.1**	*-0.0*	**1.5**	*0.9*	*-0.3*
Ilulissat						*-0.3*		*1.8*	*-1.1*			
Sisimiut			*-1.3*			*-0.8*			*0.1*			*-1.5*
Kangerlussuaq	**4.3**	*2.6*	*-0.9*	**3.5**	*1.9*	*0.8*	**2.0**	*1.4*	*0.6*	*1.1*	*-0.5*	*-1.4*
Nuuk						*0.5*	**3.4**	**3.4**	*1.4*	**1.6**	*1.2*	*-0.9*
Narsarsuaq	**3.9**	**4.0**	*-0.9*	**3.6**	*2.2*	*-0.7*	**2.7**	**1.9**	*0.5*	**1.8**	*1.2*	*-0.4*
Danmarkshavn								*1.6*	*0.6*			
CGT2	*2.6*	**2.9**	*-1.1*	*1.9*	*2.0*	*-0.3*	**2.2**	**1.9**	*-0.0*	*0.9*	*0.8*	*-0.6*
CGT3	*0.7*	*2.1*	*-0.7*	*0.7*	*1.8*	*0.7*	**1.9**	**2.0**	*0.4*	*0.3*	*0.7*	*-0.3*

Notes: Significant trends of $p \leq 0.05$ (≤ 0.01) are in bold (bold + underline). Units are °C for the specified period. Trends that are not significant are shown in italic.

TABLE 4   Seasonal trends in Greenland *mean minimum* (DMI parameter 121) daily air temperature at DMI coastal stations and CGT averages for various periods to 2019

Station WMO code	DJF (1981–2019)	DJF (1991–2019)	DJF (2001–2019)	MAM (1981–2019)	MAM (1991–2019)	MAM (2001–2019)	JJA (1981–2019)	JJA (1991–2019)	JJA (2001–2019)	SON (1981–2019)	SON (1991–2019)	SON (2001–2019)
Aasiaat	**8.3**	**7.0**	*-1.0*	**7.0**	**5.5**	*-0.5*	**3.1**	**2.4**	*0.2*	**2.2**	**1.5**	*-0.4*
Ilulissat			*-0.6*			*0.1*			*-0.4*		*-0.2*	*-0.6*
Sisimiut			*-1.5*			*-1.1*			*-1.0*			*-1.4*
Kangerlussuaq	**4.9**	*3.2*	*-1.4*	**4.4**	*3.3*	*0.5*	**1.0**	*0.6*	*-0.4*	*1.4*	*-0.0*	*-1.2*
Nuuk				*2.1*	*1.0*	*-1.3*	**2.2**	**1.7**	*-0.0*	**1.4**	*0.4*	*-1.1*
Narsarsuaq	**3.9**	**4.7**	*-0.7*	**3.4**	*2.1*	*-0.2*	*0.5*	*0.3*	*0.2*	*0.8*	*0.9*	*-0.5*
CGT2	**3.5**	**3.9**	*-0.8*	**2.5**	**2.3**	*0.0*	**1.9**	**1.4**	*-0.0*	**1.2**	*0.9*	*-0.3*
CGT3	*1.1*	*2.7*	*-0.8*	*0.6*	*1.6*	*0.7*	**1.1**	**1.0**	*0.2*	*0.4*	*0.5*	*-0.3*

Notes: Significant trends of $p \leq 0.05$ (≤ 0.01) are in bold (bold + underline). Units are °C for the specified period. Trends that are not significant are in italic.

FIGURE 5 Greenland seasonal temperature trends from MAR for (a–d) 1991–2019 (1990–2018 for autumn) and (e–h) 2001–2019 (2000–2018 for autumn). Panels (a–d) are overlain with circles representing corresponding seasonal temperature trends for DMI coastal met stations, with crosses indicating statistically-significant trends at $p \leq 0.05$ [Colour figure can be viewed at wileyonlinelibrary.com]
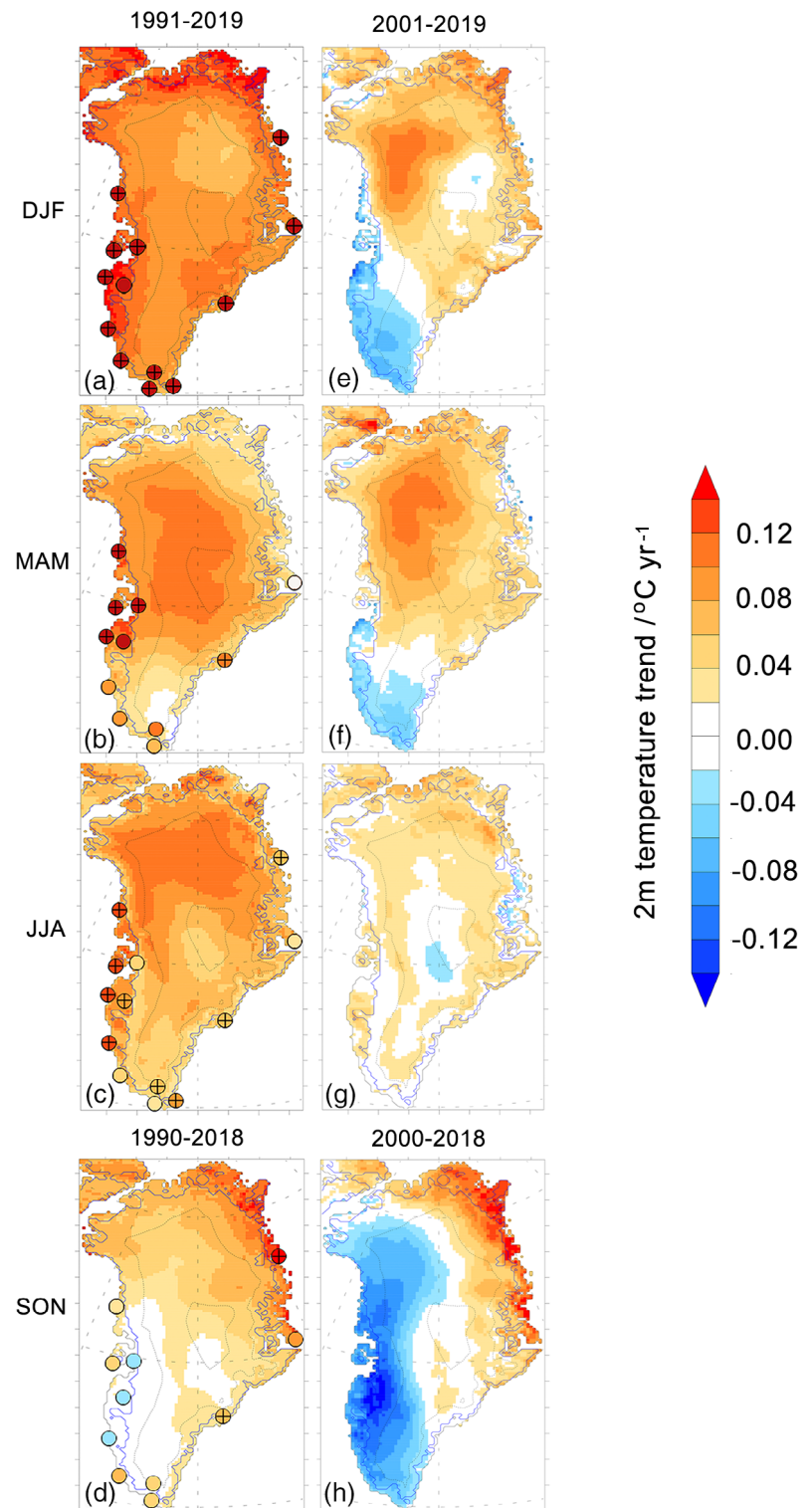
temperature maxima. This is supported by the results of Hofer *et al.* (2017) who found an effect of decreasing cloud cover in summer and the resulting increased short-wave radiation in driving GrIS mass loss between 1995 and 2009. Conversely, winter trends since 1981 and 1991 tend to be greater during the night than day. This suggests an enhanced role of cloud cover in restricting

coastal night-time cooling under a warming climate. One DMI station, Sisimiut cooled significantly in autumn during 2001–2018 in both these parameters but not in its overall mean temperature.

We also present spatial patterns of Greenland temperature trends based on the MAR model output, which indicates the regional focus of the strongest warming

shifted according to season: thus for 1991–2019 it was focused along the southwest and northern margins of the country in winter, in central Greenland and pockets along the west and northwest coast in spring, in central northern i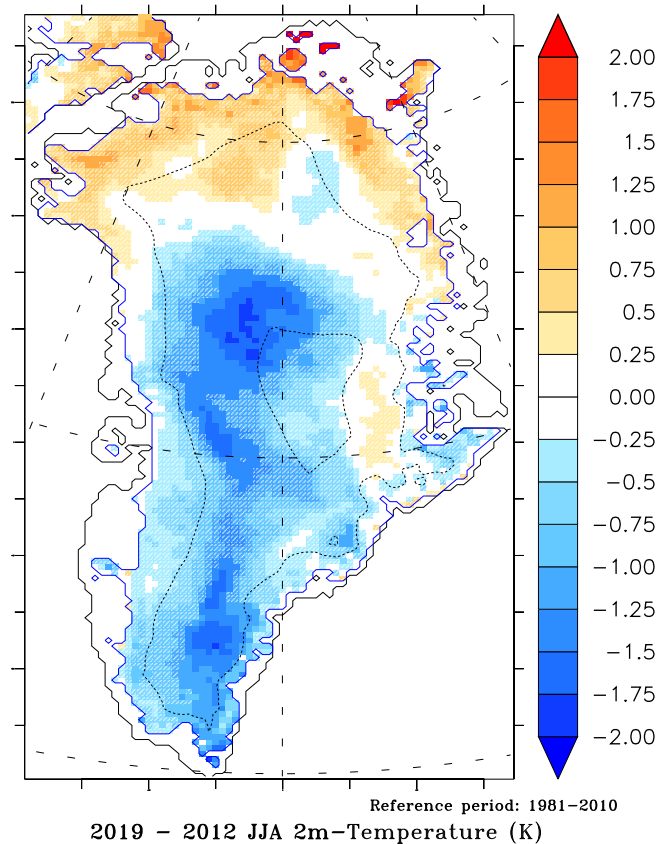nterior districts in summer, and in a narrow band along the northeast margin in autumn (Figure 5). According to MAR, and in line with the DMI coastal station analysis above, much of southern and southwest Greenland has not warmed during autumn since 1991. MAR trends between 2001 and 2019 show the southwest of the country cooling in winter and spring, and deeper, much more widespread cooling in west Greenland in autumn (Figure 5). This reflects lower geopotential heights centred in a band between southeast and northwest Greenland, which caused the advection of relatively cold air from the north and inland over the ice sheet down the west side of Greenland during the last decade in autumn (not shown).

3.2 | Relation between Greenland temperature and atmospheric circulation

Correlation coefficients between de-trended seasonal time series of Greenland coastal temperature changes and NAO changes are mainly significant and are strongest in autumn and winter and in southern Greenland (Table S1). These correlations are fairly stable through time in winter and summer but increase (decrease) for the most recent periods in spring (autumn). Although individual stations′ correlations tend to be stronger in winter, the strongest overall correlations for the CGT2/3 station averages with NAO are in both autumn (1961–90) and winter (1991–2018) for CGT2 and in autumn (1961–90) for CGT3. We also note clusters of non-significant correlations between Greenland coastal temperature and NAO: this is the case especially for Tasiilaq in spring and (mainly) summer, as well as for Upernavik, Aasiaat, Ilulissat and Sisimiut in spring when overall correlations are also weakest.

Correlations between de-trended seasonal series of Greenland coastal temperatures and GBI are nearly all significant (except for Tasiilaq), stronger than NAO
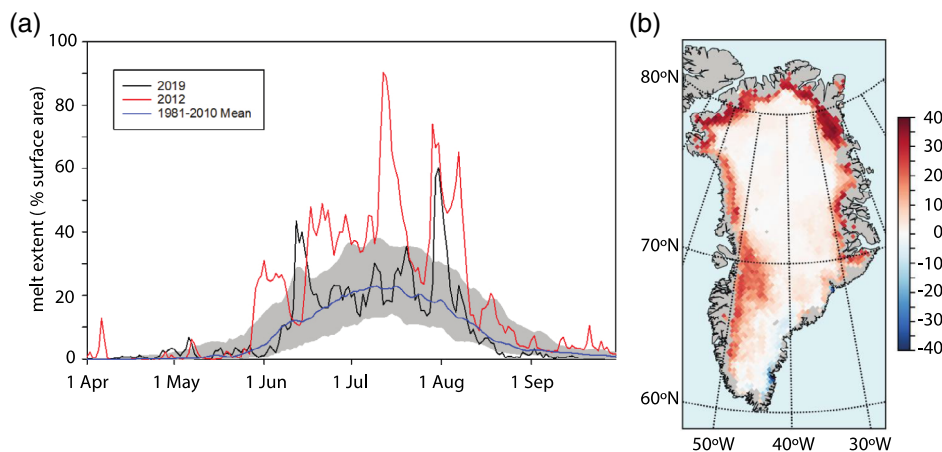

FIGURE 6 Difference in Greenland summer (JJA) temperature (°C) between 2019 and 2012 (2019 minus 2012) from MAR. Areas where the difference is less than the JJA near-surface temperature interannual variability, as represented by the standard deviation, over 1981 to 2010, are not hatched [Colour figure can be viewed at wileyonlinelibrary.com]

FIGURE 7 Greenland Ice Sheet melt extent for: (a) 2019 (black) compared with 2012 (red) and 1981–2010 mean (blue) and interdecile range (grey); and (b) melt day anomaly for 1 June to August 31, 2019 compared to 1981–2010 mean. Graphics adapted from https://nsidc.org/greenland-today/ [Colour figure can be viewed at wileyonlinelibrary.com]

FIGURE 8 Greenland Blocking Index (GBI) daily values in summer (here 1 May–31 August) for (a) 2012 and (b) 2019. The 1951–2000 day of year (DOY) GBI mean values are overplotted in (a) and (b) for reference (daily anomaly = 2012/2019 daily value–DOY mean). Plot (c) shows the total number of positive GBI daily anomalies from 1948 to 2019 inclusive for the 26 April–25 August period [Colour figure can be viewed at wileyonlinelibrary.com]
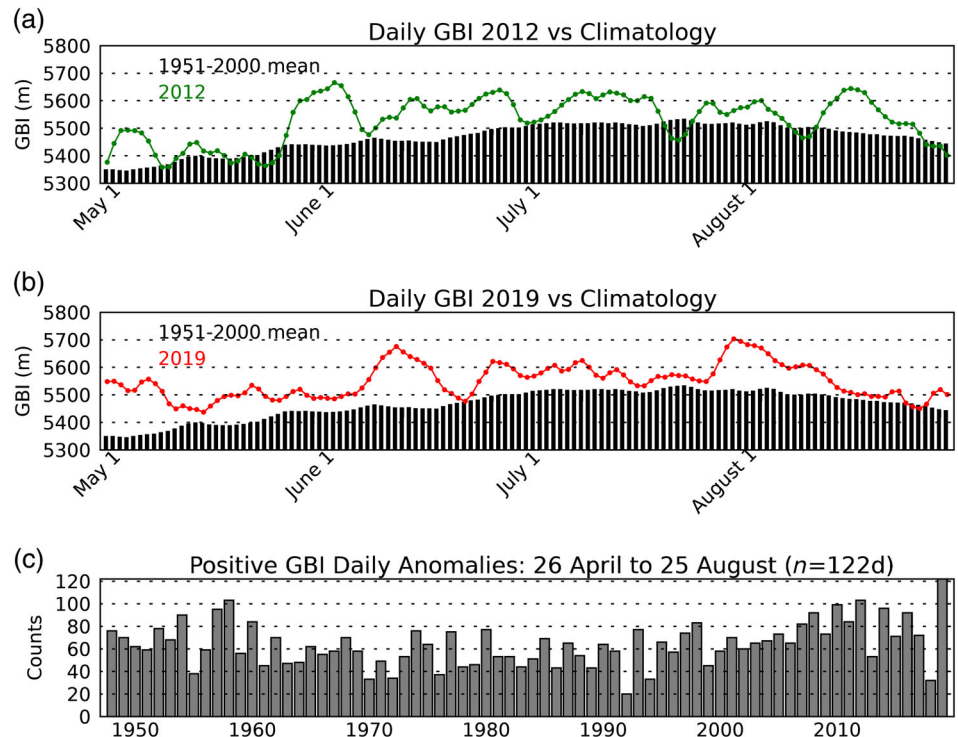
correlations, and are strongest in winter, when they peak at 0.86 for CGT2 (CGT3) (Table S2). Spring and summer temperature-GBI correlations increase through time to peak at ∼0.8 for 1991–2018. Temperature-GBI correlations peak spatially in west and south Greenland.

3.3 | Case study: summer 2019 Greenland heatwave and extreme melt event and comparison with 2012

Mean summer and July temperatures in 2019 were in the top 4–6 warmest years on record but were generally not as high as in 2012 except in northern parts of the GrIS. Summer 2019 at 7.7°C was the fourth warmest coastal Greenland summer in the CGT2 record after 2012 (8.2°C), 2010 (8.1°C) and 2003 (7.8°C), and CGT3 in 2019 at 7.8°C was the joint sixth warmest summer but both of these composite 2019 temperatures were 0.5–0.6°C below the 2012 mean summer values. July 2019 was the joint fourth warmest in both the CGT2 and CGT3 series, but was 0.9°C and 0.7°C, respectively, below the record 2012 July mean temperatures. At the time of writing, 2019 summer data were not available from Summit and Swiss Camp CG-Net AWSs. Of earlier years, 2012, closely followed by 2010 for summer, remains the warmest summer and July on record at Summit (Figure 4). At NOAA GEOSummit, which is probably the highest-quality Summit temperature record because it utilizes ventilated thermometers although its record only

begins in 2008 (Hanna et al., 2014), the summer 2019 mean temperature was −13.4°C, 0.5°C below that for summer 2012, although the July 2019 mean of −10.2°C comfortably exceeded the −11.1°C July 2012 mean temperature. For Swiss Camp (Figure 3), the summer 2012 mean temperature of +1.2°C tied with 2007 and was closely followed by 2010 at +1.1°C, while 2.0°C in July 2012 was only the second warmest July mean temperature after 2.2°C in July 2011. At Mittivakkat Gl. Nunatak (record since 1994), 2019 at 6.3°C was only the sixth highest year in the summer mean temperature series, behind 2012 at 6.7°C and well behind the warmest summers in 2005 (7.9°C) and 2010 (7.3°C).

Extreme maximum daytime temperatures in summer 2019 were also generally high but not exceptional. For example 23.4°C at Narsarsuaq on August 1, 2019 tied with 2016 as the joint fourth highest August temperature since 1961 but higher August maxima, of 24.0°C in 1966 and 23.9°C in 1987, were recorded at that station before the recent major warming period in the 2000s. An absolute maximum temperature of 20.0°C at Ilulissat in July 2019 was the joint sixth highest on record (records since 1890), recently exceeded by 21.1°C in 2012 and 21.7°C in 2017, although 21.9°C was recorded there in July 1908. However, at Danmarkshavn, on the north-east Greenland coast (Figure 1), the August 2019 maximum of 19.7°C was nearly 2°C above the next warmest August maximum of 17.8°C in 2012 (based on records back to 1949). Perhaps most notably, there was a new record absolute maximum temperature of 1.2°C at NOAA

GEOSummit on July 31, 2019, which slightly exceeded the previous daily maximum record of 1.0°C recorded there on July 11, 2012 (Hanna et al., 2014; NSIDC, 2019). However, summer 2019 absolute maximum temperatures at Nuuk, Ittoqqortoormiit and Tasiilaq were unremarkable. This analysis based on coastal AWS data is confirmed by plots from MAR comparing temperature differences for summer 2019 versus 2012, where only northernmost Greenland was generally warmer, by up to ∼2°C, in 2019 (Figure 6).

There is a well-established highly significant correlation between Greenland temperature and melt (Hanna et al., 2008; Hanna et al., 2013b). According to 1950–2019 MAR model outputs forced by NCEP-NCARv1, increasing GrIS summer mean temperature by 1°C results in 126.9 Gt·yr^{-1} extra generation of summer meltwater production ($r = 0.89$) and a correspondingly greater monthly sum of daily melt areas of 7.748×10^6 km^2 (6.490×10^6 km^2) for a surface meltwater production threshold of >1 (>5) mm·day^{-1} (respective r values of 0.91 and 0.88). Estimates of the spatial extent of melt in late July 2019 exceeded any date since July 2012 (Figure 7a). The extent reached a maximum of 60.3% on July 31, 2019, compared to an average (1981–2010) maximum extent of 39.8%. The surface melt extent on 30 July was the first time that melt was detected at the highest elevation of the ice sheet, Summit Station, since July 11, 2012. The 2019 melt duration, which is calculated as the number of days with melt detected for a given 25-km grid cell, exceeded the mean across most of the ice sheet. The entire northern periphery of the ice sheet had at least 20 more days with melt, in some locations nearly 50 more days with melt, compared to the mean (Figure 7b). Only a thin elevation band along the southeastern margin had below-average melt (Figure 7b).

The warm Greenland summers of 2012 and 2019 were characterized by high-pressure blocking that promoted the advection of warm air masses from further south. In 2019, peak Greenland blocking occurred during 10–17 June (with the GBI value peaking at +2.96σ above the 1951–2000 mean on 12 June), 9 July (GBI of +2.05σ), and 30 July to 4 August (peak GBI of +3.04σ on 31 July), when the GBI was >2σ above the respective daily long-term means. In summer 2012, peak GBI was on 31 May to 5 June (peaking at 2.76σ on 3 June), 14–15, 18 and 27 June (2.39σ on 15 June), 9–10 and 13 July (2.21σ on 9 July), and 16–19 August (peaking at 2.56σ on 17 August). Summers 2012 and 2019 both had a total of 16 days with the GBI > +2σ; however, 2019 had greater extremes (∼+3σ) in daily GBI, marked by several consecutive days of +100 m geopotential height anomalies (Figure 8a,b). Figure 8c shows the total number of positive GBI days since 1948 for the 26 April – 25 August
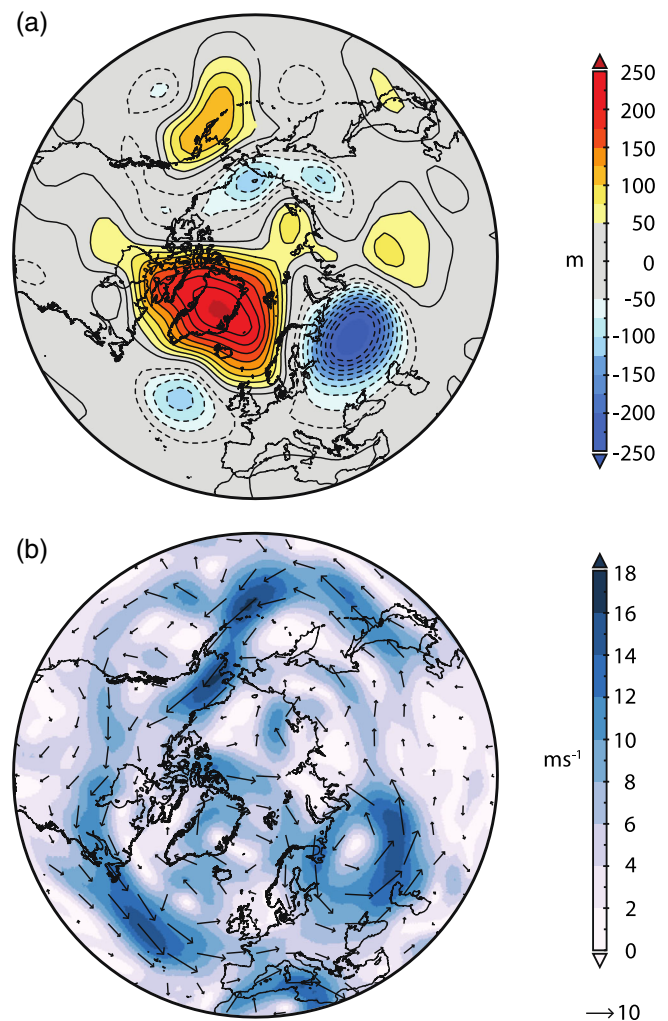
FIGURE 9 NCEP/NCAR Reanalysis v1 mean (a) 500 hPa geopotential anomalies and (b) 700 hPa vector winds indicating direction of anomalous south-easterly airflow over Greenland during the high Greenland Blocking (GB) and high ice-melt episode from 30 July to August 4, 2019, during which consecutive daily GB anomalies were all >2σ. For panel (a) negative contours are dotted and the zero contour is omitted [Colour figure can be viewed at wileyonlinelibrary.com]

period. This set of dates reflects the remarkable window in 2019 of 122 consecutive positive GBI days spanning most of the melt season, while 1958 and 2012 – each with 103 days – have the second greatest number of positive GB days over this period.

There are fundamental differences in the synoptic causes of the mid-July 2012 and end of July 2019 high melt episodes. In 2012, high Greenland blocking led to a relatively warm south-westerly airstream being advected up over the western flank of the GrIS and producing the record melt (Nghiem et al., 2012; Hanna et al., 2014), while in 2019 a prevailing easterly airflow arising from low pressure over the northeast North Atlantic caused a
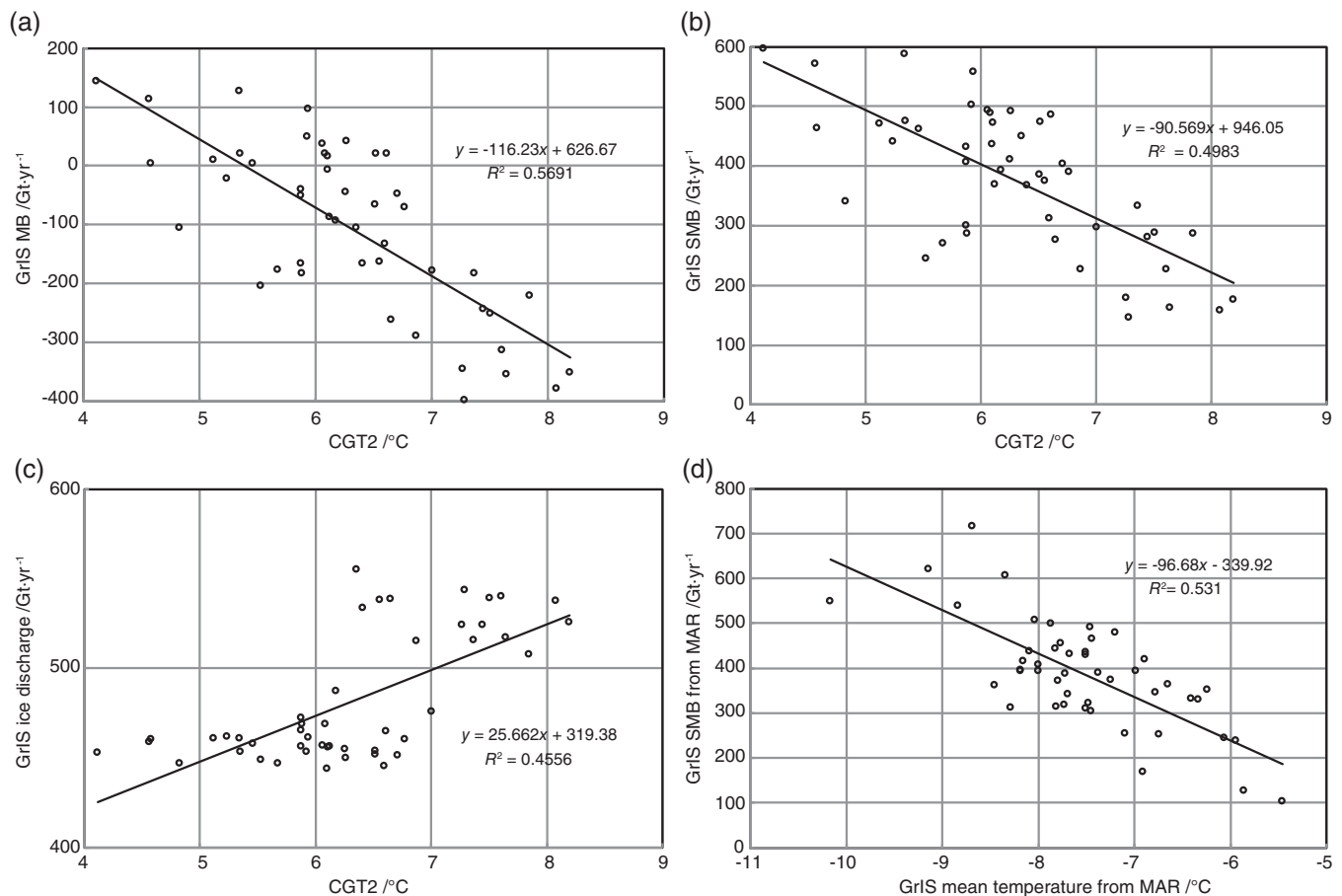
FIGURE 10 Modelled GrIS annual (a) total mass balance, (b) surface mass balance and (c) ice discharge versus summer Composite Greenland Temperature 2 (CGT2 is a 9-station average; see Section 2 for definition). For comparison with (b), graph (d) shows MAR/NCEP-modelled GrIS annual SMB versus mean GrIS summer temperature (see main text, Section 3.4, for discussion). All relations are built using 1972–2018 data. Mass balance model output for (a–c) are from Mouginot *et al.* (2019)

relatively warm airmass to be advected westwards over the southeastern flank of the ice sheet and then subside down the western side where it further warmed adiabatically (NSIDC, 2019) (Figure 9) Once again this resulted in extreme surface melt, although overall not as extreme as in 2012, and is considered to have resulted in an exceptionally prolonged period of above-freezing temperatures at Summit (NSIDC, 2019).

3.4 | Observed and model predicted relationships between GrIS mass balance and air temperatures

Summer means (1972–2018) of Greenland CGT2 coastal temperatures and MAR-modelled whole GrIS temperatures are very strongly correlated at $r = 0.84$, where a 1°C change in CGT2 corresponds to a 0.81°C change in the mean temperature of the Greenland ice sheet and peripheral glaciated areas. Based on years 1972–2018, summer CGT2 data are significantly correlated with GrIS total

mass balance (MB), surface mass balance and ice discharge annual data from Mouginot *et al.* (2019) (Figure 10). CGT2 explains the following variance in MB, SMB and discharge (respectively 57%, 50% and 46%). From these linear fits we infer that a 1°C increase in Greenland coastal summer temperature equates to a 116.2 Gt·yr^{-1} decrease in MB, which for this temperature change consists of a 90.6 Gt·yr^{-1} decrease in SMB, and a 25.7 Gt·yr^{-1} increase in discharge. Neglecting other factors such as precipitation changes, which are very much second-order in recent decades (e.g., Wilton *et al.*, 2017), this implies that 78 (22)% of the ice sheet's recent response to changing surface air temperatures has been via SMB (dynamical) changes. Comparing NCEP (ERA)-driven MAR output of annual SMB plotted against whole GrIS summer temperature gives a similar correlation, with an explained variance of 53 (58) %, while a 1°C change in GrIS area-average summer temperature corresponds to a similar 96.7 (114.1) Gt·yr^{-1} decline in SMB.

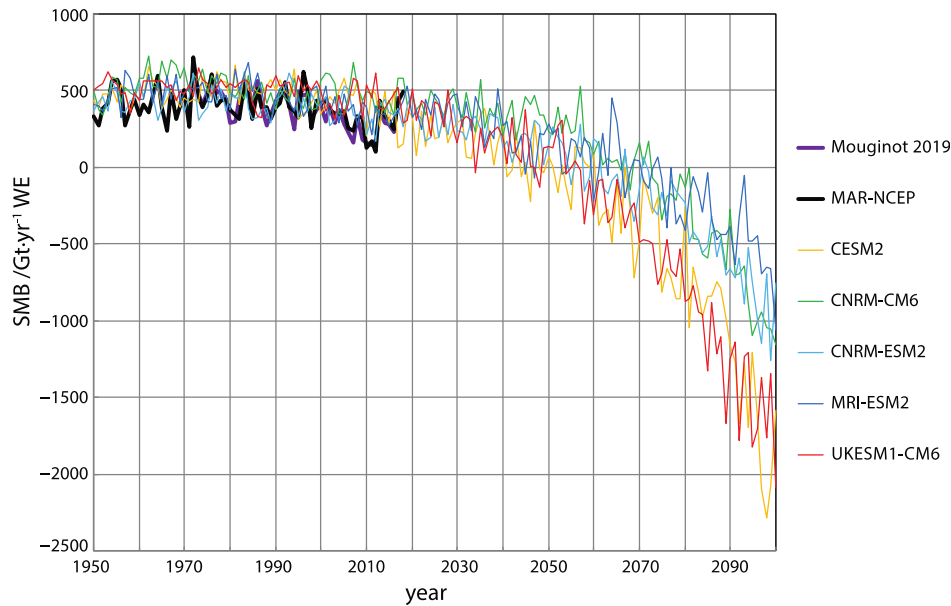Our five CMIP6 model runs under the SSP5-8.5 scenario provide a mean summer warming of 5.3°C (range

FIGURE 11 Greenland Ice Sheet annual SMB after Mouginot *et al.* (2019) (purple line), based on the RACMO regional climate/SMB model, and as simulated by MAR using NCEP-NCAR v1 Reanalysis data from 1950–2018 (black line) and MAR runs using five different CMIP6 GCMs (MAR-CESM2, MAR-CNRM-CMIP6, MAR-CNRM-ESM2, MAR-MRI-ESM2, MAR-UKESM1-CMIP6) and the SSP5-8.5 scenario as forcing (other colour lines) (Hofer *et al.*, in review). Note this does not include topographic changes or surface-elevation feedbacks, which would likely increase the changes shown here, especially after 2070 [Colour figure can be viewed at wileyonlinelibrary.com]
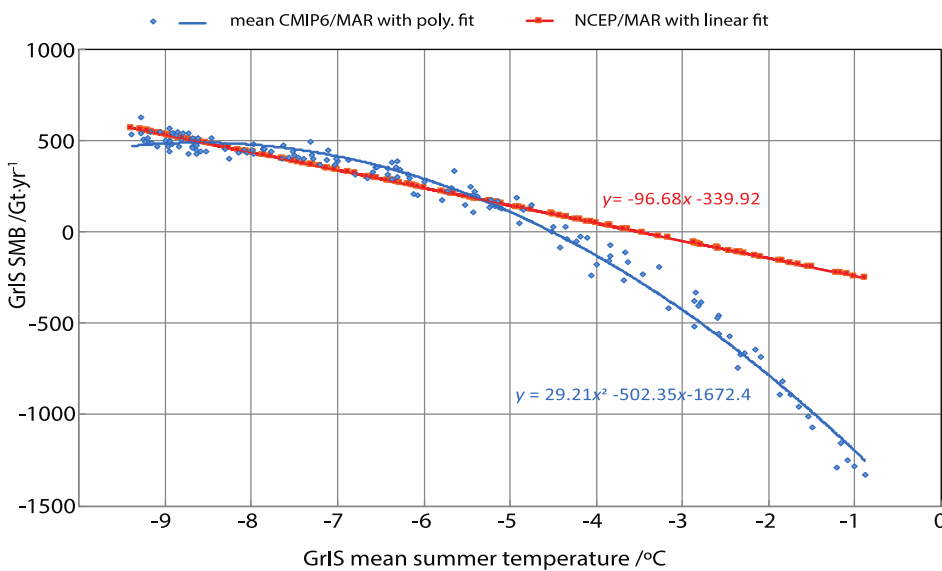
FIGURE 12 Sensitivity of GrIS SMB simulated by MAR and CMIP6 (mean of five models named in Section 2) to GrIS mean summer temperature over the period 1950–2100 (diamonds with blue quadratic polynomial line fitted through). For comparison, the relations we previously develop based on MAR simulations for 1972–2018 are shown by the red squares and line (linear regression; Figure 10d), discussed in Section 3.4 [Colour figure can be viewed at wileyonlinelibrary.com]

4.0–6.6°C) for 2081–2099 relative to 2001–2019 (Table 1). According to our linear relations above based on Mouginot *et al.* (2019) and weather station data, this is likely to result in a SMB decrease of 362.4–598.0 (mean 480.2) Gt·yr^{-1} by 2081–2099: and a resulting 1.00–1.65 mm·yr^{-1} increased contribution of the GrIS to global sea-level rise [in addition to its recent contribution of 0.75 mm·yr^{-1} reported by Mouginot et al. (2019) for 2001–2018], which represents an approximate doubling

of the recent (1990s to present) rate of GrIS mass loss (Bamber *et al.*, 2018; Hanna *et al.*, 2020). Assuming linearity (which is a simplistic assumption because the rate of decline of SMB is likely to accelerate markedly during the late 21st century, especially during the last decade; Figure 11), this would give a corresponding GrIS global sea-level (GSL) contribution of ~10.0–12.6 cm by 2100 relative to 2020. Although we do not extrapolate recent MB and discharge trends to 2100, due to unclear causal

relations between air temperature and solid-ice discharge, it is possible that increasing discharge in a warmer climate (Bigg *et al.*, 2014) may add to accelerating GSL contribution from greater SMB losses.

Our extrapolation of future GrIS SMB change is likely conservative and limited by the following factors:

1. It is derived using data from a period from which we know that not all SMB change was temperature-driven, being augmented by changes in atmospheric circulation, warm-air advection and reduced albedo (Pattyn *et al.*, 2018). In our temperature-SMB correlation, the entire energy balance (and energy excess for melt) is expressed in terms of temperature, whereas there is an important radiation-related, temperature-independent contribution to the SMB decrease. Therefore, the relation between SMB and temperature over recent decades may vary from the longer term.
2. It does not take into account the findings of Fettweis *et al.* (2013) and Trusel *et al.* (2018) on the quadratic relation between summer temperature and melt/runoff, and therefore SMB and MB. Our GrIS SMB projection based on recent (1972–2018) climatic conditions severely underestimates the rate of future change according to the mean SMB changes simulated by MAR forced by the five CMIP6 models we use here (Figure 12).
3. We also assume that there is no change in the ice-sheet topography (Le clec'h *et al.*, 2019) or dynamical mass losses.

Nevertheless, despite the above limitations, our simple calculation supports the dominant role of SMB changes (Goelzer *et al.*, 2013) in the 8–27 cm "likely range" (mean 15 cm) total GrIS sea-level commitment under RCP8.5 reported by IPCC (2019, SPM.B1.2).

4 | CONCLUSIONS

Our updated analysis of Greenland coastal and inland weather station records shows strong and significant warming since 1991 in all seasons ($\sim$1.7°C in summer and $\sim$4.4°C in winter), where the summer warming compares well between coastal and inland (Swiss Camp, Summit) sites; however, trend analysis for 2001–2019 highlights compensating short-term warming and cooling before and after 2012 that gives no significant net temperature change at most stations. However, flatter or slightly declining temperature trends for some sites since around 2010 are generally insignificant and well within the scope of natural variability. Summer 2019 saw near-record warmth and melt but was not quite as warm as summer 2012 over most of Greenland except at Summit and in the north; however, summer 2019 had a record number of blocked days over Greenland, and was notable for its peak warmth and melt (31 July) occurring relatively late in the melt season, which also coincided with the date of peak blocking. By quantifying the relation between observed and projected Greenland surface air temperature changes and modelled GrIS mass balance changes, we have underscored the likely high sensitivity of the GrIS to continued global warming, and have provided some initial predictions of GrIS SMB change. We have also quantified a highly significant ($r \sim 0.8$) association between coastal Greenland mean surface air temperatures and GBI variations, which has increased in strength in spring and summer in recent decades. One of the main causes of blocking is surface warming and consequent warming of the tropospheric air column, but increased blocking also enhances summer warming through warm-air advection and decreased cloud cover. This makes it crucial to improve the understanding and currently questionable predictions of future trends in Greenland regional atmospheric circulation, especially blocking (e.g., Hanna *et al.*, 2018b), when attempting to decipher ice-sheet "weather" from "climate" and, in particular, to quantify the effects of continued global warming on GrIS mass balance.

ORCID
Edward Hanna https://orcid.org/0000-0002-8683-182X
Sebastian H. Mernild https://orcid.org/0000-0003-0797-3975
Thomas J. Ballinger https://orcid.org/0000-0002-8722-1927
Richard J. Hall https://orcid.org/0000-0003-4840-383X

REFERENCES

Abermann, J., Hansen, B., Lund, M., Wacker, S., Karami, M. and Cappelen, J. (2017) Hotspots and key periods of Greenland climate change during the past six decades. *Ambio*, 46(Suppl. 1), S3–S11.

Ballinger, T.J., Hanna, E., Hall, R.J., Miller, J., Ribergaard, M.H. and Høyer, J.L. (2018) Greenland coastal air temperatures linked to Baffin Bay and Greenland Sea ice conditions during autumn through regional blocking patterns. *Climate Dynamics*, 50, 83–100.

Bamber, J.L., Westaway, R.M., Marzeion, B. and Wouters, B. (2018) The land ice contribution to sea level during the satellite era. *Environmental Research Letters*, 13, 063008.

Bigg, G.R., Wei, H.-L., Wilton, D.J., Zhao, Y., Billings, S.A., Hanna, E. and Kadirkamanathan, V. (2014) A century of variation in the dependence of Greenland iceberg calving on ice sheet surface mass balance and regional climate change. *Proceedings of the Royal Society A*, 470, 20130662.

Box, J.E., Colgan, W.T., Wouters, B., Burgess, D.O., O'Neel, S., Thomson, L.I. and Mernild, S.H. (2018) Global sea-level contribution from Arctic land ice: 1971-2017. *Environmental Research Letters*, 13, 125012.

Cappelen, J. (Ed.). (2020) *Greenland – DMI Historical Climate Data Collection 1784–2019. DMI Report 20-04*. Copenhagen: Danish Meteorological Institute. https://www.dmi.dk/publikationer/.

Delhasse, A., Fettweis, X., Kittel, C., Amory, C. and Agosta, C. (2018) Brief communication: Impact of the recent atmospheric circulation change in summer on the future surface mass balance of the Greenland Ice Sheet. *The Cryosphere*, 12, 3409–3418.

Delhasse, A., Kittel, C., Amory, C., Hofer, S. and Fettweis, X. (2020) Brief communication: Evaluation of the near-surface climate in ERA-5 over the Greenland ice sheet. *The Cryosphere*, 14, 957–965.

Fettweis, X., Franco, B., Tedesco, M., van Angelen, J.H., Lenaerts, J.T.M., van den Broeke, M.R. and Gallée, H. (2013) Estimating the Greenland ice sheet surface mass balance contribution to future sea level rise using the regional atmospheric climate model MAR. *The Cryosphere*, 7, 469–489.

Fettweis, X., Box, J.E., Agosta, C., Amory, C., Kittel, C., Lang, C., van As, D., Machguth, H. and Gallée, H. (2017) Reconstructions of the 1900–2015 Greenland ice sheet surface mass balance using the regional climate MAR model. *The Cryosphere*, 11, 1015–1033.

Fettweis, X., Hofer, S., Krebs-Kanzow, U., Amory, C., Aoki, T., Berends, C.J., Born, A., Box, J.E., Delhasse, A., Fujita, K., Gierz, P., Goelzer, H., Hanna, E., Hashimoto, A., Huybrechts, P., Kapsch, M.-L., King, M.D., Kittel, C., Lang, C., Langen, P.L., Lenaerts, J.T.M., Liston, G.E., Lohmann, G., Mernild, S.H., Mikolajewicz, U., Modali, K., Mottram, R.H., Niwano, M., Noël, B., Ryan, J.C., Smith, A., Streffing, J., Tedesco, M., van de Berg, W.J., van den Broeke, M., van de Wal, R.S.W., van Kampenhout, L., Wilton, D., Wouters, B., Ziemen, F. and Zolles, T. (2020) GrSMBMIP: Intercomparison of the modelled 1980–2012 surface mass balance over the Greenland Ice sheet. *The Cryosphere Discussions*. https://doi.org/10.5194/tc-2019-321.

Goelzer, H., Huybrechts, P., Fürst, J.J., Andersen, M.L., Edwards, T.L., Fettweis, X., Nick, F.M., Payne, A.J. and Shannon, S.R. (2013) Sensitivity of Greenland ice sheet projections to model formulations. *Journal of Glaciology*, 59, 733–749. https://doi.org/10.3189/2013JoG12J182.

Hanna, E. and Cappelen, J. (2002) Recent climate of southern Greenland. *Weather*, 57, 320–328.

Hanna, E. and Braithwaite, R. (2003) The Greenland ice sheet: a global warming signal? *Weather*, 57, 351–357.

Hanna, E., Mernild, S.H., Cappelen, J. and Steffen, K. (2012) Recent warming in Greenland in a long-term instrumental (1881-2012) climatic context. I. Evaluation of surface air temperature records. *Envionmental Research Letters*, 7, 045404.

Hanna, E., Navarro, F.J., Pattyn, F., Domingues, C.M., Fettweis, X., Ivins, E.R., Nicholls, R.J., Ritz, C., Smith, B., Tulaczyk, S., Whitehouse, P.L. and Zwally, H.J. (2013a) Ice-sheet mass balance and climate change. *Nature*, 498, 51–59.

Hanna, E., Jones, J.M., Cappelen, J., Mernild, S.H., Wood, L., Steffen, K. and Huybrechts, P. (2013b) The influence of North Atlantic atmospheric and oceanic forcing effects on 1900-2010 Greenland summer climate and ice melt/runoff. *International Journal of Climatology*, 33, 862–880.

Hanna, E., Fettweis, X., Mernild, S.H., Cappelen, J., Ribergaard, M.H., Shuman, C.A., Steffen, K., Wood, L. and Mote, T.L. (2014) Atmospheric and oceanic climate forcing of the exceptional Greenland ice sheet surface melt in summer 2012. *International Journal of Climatology*, 34, 1022–1037.

Hanna, E., Cropper, T.E., Hall, R.J. and Cappelen, J. (2016) Greenland Blocking Index 1851-2015: a regional climate change signal. *International Journal of Climatology*, 36, 4847–4861.

Hanna, E., Hall, R.J., Cropper, T.E., Ballinger, T.J., Wake, L., Mote, T. and Cappelen, J. (2018a) Greenland blocking index daily series 1851-2015: analysis of changes in extremes and links with North Atlantic and UK climate variability and change. *International Journal of Climatology*, 38, 3546–3564.

Hanna, E., Fettweis, X. and Hall, R.J. (2018b) Brief communication: Recent changes in summer Greenland blocking captured by none of the CMIP5 models. *The Cryosphere*, 12, 3287–3292.

Hanna, E., Pattyn, F., Navarro, F., Favier, V., Goelzer, H., van den Broeke, M.R., Vizcaino, M., Whitehouse, P.L., Ritz, C., Bulthius, K. and Smith, B. (2020) Mass balance of the ice sheets and glaciers – progress since AR5 and challenges. *Earth Science Reviews*, 201, 102976.

Hofer, S., Tedstone, A.J., Fettweis, X. and Bamber, J.L. (2017) Decreasing cloud cover drives the recent mass loss on the Greenland Ice Sheet. *Science Advances*, 3(6), e1700584.

Hofer, S., Lang, C., Amory, C., Kittel, C., Delhasse, A., Tedstone, A., Alexander, P.M., Smith, R. and Fettweis, X. (in review) Doubling of future Greenland Ice Sheet surface melt revealed by the new CMIP6 high-emission scenario. *Nature Communications*.

Hurrell, J.W. (1995) Decadal trends in the North Atlantic Oscillation: regional temperatures and precipitation. *Science*, 269, 676–679.

IPCC. (2019) Summary for policymakers. In: Pörtner, H.-O., Roberts, D.C., Masson-Delmotte, V., Zhai, P., Tignor, M., Poloczanska, E., Mintenbeck, K., Nicolai, M., Okem, A., Petzold, J., Rama, B. and Weyer, N. (Eds.) *IPCC Special Report on the Ocean and Cryosphere in a Changing Climate*. Intergovernmental Panel on Climate Change, https://report.ipcc.ch/srocc/pdf/SROCC_SPM_Approved.pdf.

Le clec'h, S., Charbit, S., Quiquet, A., Fettweis, X., Dumas, C., Kageyama, M., Wyard, C. and Ritz, C. (2019) Assessment of the

Greenland ice sheet–atmosphere feedbacks for the next century with a regional atmospheric model coupled to an ice sheet model. *The Cryosphere*, 13, 373–395.

Lenton, T.M., Held, H., Kriegler, E., Hall, J.W., Lucht, W., Rahmstorf, S. and Schnellnhuber, H.J. (2008) Tipping elements in the Earth's climate system. *Proceedings of the National Academy of Sciences*, 105, 1786–1793.

Maslanik, J. and Stroeve, J. (1999) *Near-Real-Time DMSP SSMIS Daily Polar Gridded Sea Ice Concentrations, Version 1*. NASA National Snow and Ice Data Center Distributed Active Archive Center. Boulder, CO: National Snow and Ice Data Center. https://doi.org/10.5067/U8C09DWVX9LM.

Mernild, S.H., Hanna, E., Yde, J.C. and Malmros, J.K. (2013) Coastal Greenland air temperature extremes and trends 1890-2010: annual and monthly analysis. *International Journal of Climatology*, 34, 1472–1487.

Mote, T. (2007) Greenland surface melt trends 1973-2007: Evidence of a large increase in 2007. *Geophysical Research Letters*, 34, L22507.

Mote, T. (2014) *MEaSUREs Greenland Surface Melt Daily 25km EASE-Grid 2.0, Version 1*. Boulder, Colorado: NASA National Snow and Ice Data Center Distributed Active Archive Center.

Mote, T. and Anderson, M. (1995) Variations in melt on the Greenland ice sheet based on passive microwave measurements. *Journal of Glaciology*, 41, 51–60.

Mouginot, J., Rignot, E., Bjork, A.A., van den Broeke, M., Millan, R., Morlighem, M., Noel, B., Scheuchl, B. and Wood, M. (2019) Forty-six years of Greenland Ice Sheet mass balance from 1972 to 2018. *PNAS*, 116, 9239–9244.

Nghiem, S.V., Hall, D.K., Mote, T.L., Tedesco, M., Albert, M.R., Keegan, K., Shuman, C.A., DiGirolamo, N.E. and Neumann, G. (2012) The extreme melt across the Greenland ice sheet in 2012. *Geophysical Research Letters*, 39, L20502.

Nowicki, S.M.J., Payne, A., Larour, E., Seroussi, H., Goelzer, H., Lipscomb, W., Gregory, J., Abe-Ouchi, A. and Shepherd, A. (2016) Ice Sheet Model Intercomparison Project (ISMIP6) contribution to CMIP6. *Geoscientific Model Development*, 9, 4521–4545.

NSIDC. (2019) *Europe's warm air spikes Greenland melting to record levels. Greenland ice sheet today*. Boulder, CO: National Snow and Ice Data Center. http://nsidc.org/greenland-today/2019/08/europes-warm-air-spikes-greenland-melting-to-record-levels/.

Ogi, M., Rysgaard, S. and Barber, D.G. (2016) The influence of winter and summer atmospheric circulation on the variability of temperature and sea ice around Greenland. *Tellus A: Dynamical Meteorology & Oceanography*, 68, 31971.

O'Neill, B.C., Tebaldi, C., van Vuuren, D.P., Eyring, V., Friedlingstein, P., Hurtt, G., Knutti, R., Kriegler, E., Lamarque, J.-F., Lowe, J., Meehl, G.A., Moss, R., Riahi, K. and Sanderson, B.M. (2016) The Scenario Model Intercomparison Project (ScenarioMIP) for CMIP6. *Geoscientific Model Development*, 9, 3461–3482. https://doi.org/10.5194/gmd-9-3461-2016.

Pattyn, F., Ritz, C., Hanna, E., Asay-Davis, X., DeConto, R., Durand, G., Favier, L., Fettweis, X., Goelzer, H.,

Golledge, N.R., Munneke, P.K., Lenaerts, J.T.M., Nowicki, S., Payne, A.J., Robinson, A., Seroussi, H., Trusel, L.D. and van den Broeke, M. (2018) The Greenland and Antarctic ice sheets under 1.5°C global warming. *Nature Climate Change*, 8, 1053–1061.

Shepherd, A., Ivins, E., and Rignot, E., et al. (2020) Mass balance of the Greenland Ice Sheet from 1992 to 2018. *Nature*, 579233–239. https://doi.org/10.1038/s41586-019-1855-2.

Steffen, K. and Box, J.E. (2001) Surface climatology of the Greenland ice sheet: Greenland Climate Network 1995-1999. *Journal of Geophysical Research*, 106(D24), 33951–33964.

Tedesco, M., Fettweis, X., Mote, T., Wahr, J., Alexander, P., Box, J.E. and Wouters, B. (2013) Evidence and analysis of 2012 Greenland records from spaceborne observations, a regional climate model and reanalysis data. *The Cryosphere*, 7, 615–630.

Tedesco, M., Moon, T., Anderson, J.K., Box, J.E., Cappelen, J., Fausto, R.S., Fettweis, X., Loomis, B., Mankoff, K.D., Mote, T., Smeets, C.J.P.P., van As, D. and Van de Wal, R.S.W. (2019) *Greenland ice sheet, NOAA arctic report card 2019*. Silver Spring, MD: National Oceanic and Atmospheric Administration, Available at: https://arctic.noaa.gov/Report-Card/Report-Card-2019/ArtMID/7916/ArticleID/842/Greenland-Ice-Sheet.

Tedesco, M. and Fettweis, X. (2020) Unprecedented atmospheric conditions (1948-2019) drive the 2019 exceptional melting season over the Greenland ice sheet. *The Cryosphere*, 14, 1209–1223.

Trusel, L.D., Das, S.B., Osman, M.B., Evans, M.J., Smith, B.E., Fettweis, X., McConnell, J.R., Noel, B.P.Y. and van de Broeke, M.R. (2018) Nonlinear rise in Greenland runoff in response to post-industrial Arctic warming. *Nature*, 564, 104–108.

Turner, J., Lu, H., White, I., King, J.C., Phillips, T., Hosking, J.S., Bracegirdle, T.J., Marshall, G.J., Mulvaney, R. and Deb, P. (2016) Absence of 21st century warming on Antarctic Peninsula consistent wirh natural variability. *Nature*, 535, 411–415.

Wilton, D.J., Jowett, A., Hanna, E., Bigg, G.R., van den Broeke, M. R., Fettweis, X. and Huybrechts, P. (2017) High resolution (1 km) positive degree-day modelling of Greenland ice-sheet surface mass balance, 1870-2012 using reanalysis data. *Journal of Glaciology*, 63, 176–193.

SUPPORTING INFORMATION

Additional supporting information may be found online in the Supporting Information section at the end of this article.